33ND INTERNATIONAL COSMIC RAY CONFERENCE, RIO DE JANEIRO 2013
THE ASTROPARTICLE PHYSICS CONFERENCE

ICRC 2013

Very-high-energy gamma-ray emission from high-redshift blazars with Fermi-LAT data in the southern hemisphere

SHIMPEI TSUJIMOTO, JUNKO KUSHIDA, KYOSHI NISHIJIMA AND KAZUHITO KODANI

Department of Physics, Tokai University, Hiratsuka, Kanagawa 259-1292, Japan

shimpei.tsujimoto@gmail.com

Abstract: We searched high-redshift blazars in the southern hemisphere which seem to be detectable by the ground-based cherenkov telescopes, the H.E.S.S.- I and the Cherenkov Telescope Array (CTA). Three good very high energy candidates, PKS 0118-272 (z = 0.558), PKS 1244-255 (z = 0.633), and PKS 0454-234 (z = 1.003), were selected from the Second LAT AGN Catalog (2LAC) by analyzing Fermi-LAT 4 years data. We found that PKS 0118-272 could be detected constantly by the CTA, and PKS 0454-234 could be detected by the CTA when the target object in the bright period. Unfortunately, PKS 1244-255 is difficult to be detected by the CTA.

Keywords: Gamma rays: galaxies - Galaxies: active

1 Introduction

Very-High-Energy (VHE, energy E $>$ 100GeV) gamma rays are absorbed by the interaction with the Extra-galactic Background Light (EBL). The extent of absorption depends Energy (E), and redshift of the source (z). Specifically, the observed spectrum of the source at redshift F_{obs}(z) is expressed as equation (1).

$$F_{obs} = F_{int} \times \exp[-\tau(\mathrm{E},\mathrm{z})] \quad (1)$$

Where F_{int} is the intrinsic spectrum of the source at redshift z, $\tau(E,\mathrm{z})$ is the optical depth. The optical depth has been calculated from the EBL density model (Franceschini et al. (2008)[6], Domínguez et al. (2011)[5], and Gilmore et al. (2012)[9]). In this paper, we use the EBL density model by Domínguez et al. (2011), to estimate the amount of absorption of high-energy (HE, E $>$ 100MeV) gamma-rays.

The EBL density model is used for spectra of blazars. Blazars are a sub-class of Active Galactic Nuclei (AGN). They are characterized by double-peaked nonthermal emission with Spectral Energy Distributions (SEDs). Blazars include BL Lacertae objects (BL Lacs) and Flat Spectrum Radio Quasars (FSRQs). In addition BL Lacs include High-frequency peaked BL Lac (HBL), Intermediate-frequency peaked BL Lac (IBL) and Low-frequency peaked BL Lac (LBL). Most of the VHE gamma-ray loud blazars are near by the milky way(z $<$ 0.2). Now, z $>$ 0.5 blazar is only one, 3C279 (z = 0.536) was detected in 2006 by the MAGIC group above 80GeV [2]. The study of the High-redshift-blazars brings in the hint of the galaxy evolution, the star forming and the characterized of blazar.

The VHE gamma rays have been observed by the ground-based cherenkov telescopes, MAGIC, H.E.S.S. and VERIATS, etc. Almost all detected extragalactic VHE gamma-ray sources are blazar [1]. in the energy range from 10s of GeV to 10s of TeV [2]. The next generation ground-based cherenkov telescope, the Cherenkov Telescope Array (CTA) project, will start 2020s. The CTA foresees a factor of 5-10 improvement in sensitivity in the current VHE gamma ray domain of about 100GeV to 10s of TeV [3]. If the aperture of telescopes are more larger, telescopes get the lower energy threshold, also the number of telescopes are more bigger, the sensitivity of the CTA becomes much better one. In this paper, we use the H.E.S.S.- I and the CTA sensitivity model by Funk S., et al.(2012)[7].

We studied detection possibility of high-redshift blazars in the ground-based cherenkov telescopes from the Fermi gamma-ray data. This method has been performed in [11].

2 Data selection and data analysis

2.1 Data selection

We had considerd the redshifts listed in the Second LAT AGN Catalog (2LAC) [1] and cross-checked each selected blazar by other papers.

Redshifts of PKS 0118-272 (z = 0.558), PKS 1244-255 (z = 0.633) and PKS 0454-234 (z = 1.003) were reported by G. Vladilo, et al. (1997)[16], A. Savage, et al. (1976)[13] and M. Stickel, et al. (1989)[14], respectively. These sources were also listed in the 2LAC. The selection criteria were high redshift blazars with redshift z $>$ 0.536 (3C279), spectral index $<$ 2.0 (criteria 1), or spectral index $<$ 2.15 and integral flux $> 1.0 \times 10^{-9}$ [cm^{-2} sec^{-1}] (criteria 2).

PKS 0118-272 selected by clearing the criteria 1, PKS 1244-255 and PKS 0454-234 selected by clearing the criteria 2.

2.2 Data analysis

We analysed the Fermi pass 7 data between 2008 August 05 and 2012 August 05, using the likelihood analysis package of ScienceTools-v9r27p1. The events with photon energies in the range of 0.1-300GeV and a Region Of Interest (ROI) of 10 degree were selected for the likelihood analysis. We used "SOURCE" class ("evclass = 2") including both front and back events, because the "SOURCE" class is recommended for off-plane point source analysis by the likelihood analysis [4]. We excluded events with zenith an-

1. http://tevcat.uchicago.edu/
2. http://www.mpi-hd.mpg.de/hfm/HESS/
3. http://www.cta-observatory.org/
4. http://fermi.gsfc.nasa.gov/ssc/data/analysis/

Name	Redshift[1]	Integral Flux[1]	Index[1]
PKS 0118-272	0.588	$(4.35\pm0.26)\times10^{-9}$	1.927 ± 0.039
PKS 1244-255	0.633	$(8.74\pm0.37)\times10^{-9}$	2.102 ± 0.04
PKS 0454-234	1.003	$(2.27\pm0.054)\times10^{-8}$	2.033 ± 0.021

[1]2LAC data

Table 1: Target blazars list

gles larger than 100 degree and time intervals when the rocking angle was larger than 52 degree. The set of the instrument response functions of "P7SOURCE_V6" was applied. Models which were used in this study include the isotropic diffuse background, galactic diffuse background and the Second Fermi LAT Catalog(2FGL) sources in ROI of 10 degree centered at the position of Table 1 sources. In addition, we found several point-like sources near the target blazars with a significance level of greater than at least 3σ, which are not listed in 2FGL catalog. We summarized these *hidden* source positions in Table 2, and these were considered as point sources in our analysis.

The spectrum model was according to the 2FGL. Target blazars (Table 1) were used a Log-Parabola (LP) of the form $dN/dE = N_0(\mathrm{E/E_0})^{-(\Gamma+\beta\log(\mathrm{E/E_0}))}$, and *hidden* sources were used a simple Power Law (PL) of the form $dN/dE = N_0(\mathrm{E/E_0})^{-\Gamma}$, because LP is typically used for modeling blazar spectra. Where $N_0[\mathrm{cm^{-2}sec^{-1}MeV^{-1}}]$ is normalization parameter, E_0 [MeV] is scale parameter and Γ is spectral index. If the parameter β is zero, LP is equal to PL.

The method of analysis in this study was performed in the following procedures.
First step, we made a 4 years light curve each blazar. Second step, we looked for a bright term from light curve which was made in first step. Third step, we made a Spectrum Energy Distribution (SED) of each target blazar at a bright term with photon energies in the range of 0.1 - 20GeV (we made intrinsic spectrum). Note, the quantity of transmission in z = 1.003 and E = 20GeV is 96%, this value was big enough compared to VHE gamma ray (Cf Fig.1). Fourth step, we added an effect of the absorption by the EBL to intrinsic spectrum over 30GeV (We made absorbed spectrum). Last step, we compared the ground-based cherenkov telescopes (the H.E.S.S.-I and the CTA) with SED which we made in fourth step and investigate detection possibility in the H.E.S.S.-I and the CTA of high redshift blazars in this study.

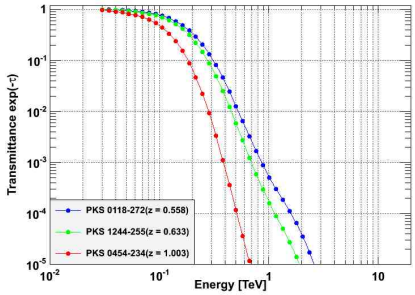

Fig. 1: Gamma ray transmissivity spectra. The EBL model is used by Domńguez et al. (2011).

3 Results and Discussion

In this section we compare the sensitivity of the H.E.S.S.-I and the CTA with results of section 2.2 and investigate the detection possibility in the H.E.S.S.-I and the CTA of high redshift blazars.

3.1 PKS 0118-272 (z = 0.558)

PKS 0118-272 (PMN J0120-2701) at z = 0.558 is the hard spectra LBL. The upper panel of Fig.2 shows a energy of 10 - 300GeV events in 0.26 degree (10GeV PSF). The bottom panel of Fig.2 shows a lightcurve of the source in the range of 0.1 - 300GeV. From Fig.2, the photons in the energy band above 10GeV are often detected regardless of brightness at 0.1GeV. The highest energy of the detected photons is 67GeV. Fig.3 shows a SED of the active period from Fig.2 (magenta region, 365days).
The best-fit parameters for the LP model between 100MeV and 20GeV during the active period are $N_0 = 0.14 \pm 0.037[10^{-9}\mathrm{cm^{-2}sec^{-1}MeV^{-1}}]$, $\Gamma = 1.38 \pm 0.17$, $\beta = 0.073 \pm 0.030$, $E_0 = 100$ [MeV]. The SED was used the long period because PKS 0118-272 is not bright at 0.1GeV. PKS 0118-272 would be possible to be detected with the CTA at any time. For reasons of the H.E.S.S.-II add a big (28m diameter) telescope to the H.E.S.S.-I. Therefore, it is difficult to detect PKS 0118-272 with the H.E.S.S.-I, but may detect it in the H.E.S.S.-II.

3.2 PKS 1244-255 (z = 0.633)

PKS 1244-255 (PMN J1246-2547) at z = 0.633 which is the soft spectra FSRQ has observed HE gamma ray active (Integral flux $> 1\times10^{-6}$) in 2009 [15]. From Fig.4, the number of photons which detected in the energy band above 10GeV increase with the active state of the 0.1-300GeV light curve. Fig.5 shows a SED of the active period from Fig.4 (magenta region, 150days). The highest energy of the detected photons is 38GeV.
The best-fit parameters for the LP model between 100MeV and 20GeV during the active period are $N_0 = 1.88 \pm 0.0085[10^{-9}\mathrm{cm^{-2}sec^{-1}MeV^{-1}}]$, $\Gamma = 1.84 \pm 0.0023$, $\beta = 0.10 \pm 8.3\times10^{-4}$, $E_0 = 100$ [MeV].
It is difficult to detect PKS 1244-255 with the CTA and the H.E.S.S.-I in the active period.

3.3 PKS 0454-234 (z = 1.003)

PKS 0454-234 (PMN J0457-2324) at z = 1.003 is the soft spectra FSRQ, however this is bright at the HE gamma ray regime (Average integral Flux is $2.82\times10^{-7}\pm1.10\times10^{-9}$ between 0.1GeV and 300GeV during 4 years). This object has observed HE gamma ray active a few times [4, 10] and it was followed up by Near Infrared (NIR) and radio [3, 12, 8]. From Fig.6, the number of photons which detected in the energy band above 10GeV increase with the active state of the 0.1-300GeV light curve. Fig.7 shows

Name	PKS 0118-272	PKS 1244-255	PKS 0454-234
source 1	(19.08,-27.77)	(198.23,-23.84)	(68.62,-23.68)
source 2	(21.35,-25.89)	(194.75,-23.22)	(70.03,-24.99)
source 3	(21.54,-22.44)	(189.33,-19.93)	(71.78,-25.67)
source 4	(19.43,-21.22)	(184.52,-24.70)	(72.19,-21.47)

Table 2: Summary of additional *hidden* source positions of the Fermi-LAT analysis (RA [degree], Dec [degree]). These sources are detected over 3σ significance levels by the 4 years data.

a SED of the active period from Fig.6 (magenta region, 100days). Though PKS0454-234 is z = 1.003, a ∼100GeV (99.4GeV) photon is detected.
The best-fit parameters for the LP model between 100MeV and 20GeV during the active period are $N_0 = 4.99 \pm 0.14[10^{-9}\mathrm{cm}^{-2}\mathrm{sec}^{-1}\mathrm{MeV}^{-1}]$, $\Gamma = 1.59 \pm 0.018$, $\beta = 0.11 \pm 0.0055$, $E_0 = 100$ [MeV].

It is difficult to detect PKS 0454-234 with the CTA and the H.E.S.S.-I at all times, however it would be possible to be detected with the CTA (and the H.E.S.S.-II) at the active period of the HE gamma rays.

Note, PKS 0454-234 would be possible to be detected with the CTA between 40GeV and 200GeV at the period between MJD 55150 and MJD 55200 (this period was detected 99.4GeV photon in ROI of 0.26 degree).

4 Cunclusion

We searched high-redshift blazars which seem to be detectable by the ground-based cherenkov telescopes, the H.E.S.S.- I and the CTA. Three good very high energy candidates, PKS 0118-272 (z = 0.558), PKS 1244-255 (z = 0.633), and PKS 0454-234 (z = 1.003), were selected from the 2LAC by analyzing Fermi-LAT 4 years data. As a result, PKS 0118-272 could be detected constantly by the CTA, and PKS 0454-234 could be detected by the CTA when the target object is in the bright period. Unfortunately, PKS 1244-255 is difficult to be detected by the CTA.

Observations with the CTA starts in the 2020s, and observations with Extreamely Large optical Telescope (ELT) starts by the 2020 [5] [6] [7]. Future observations of extragalactic blazars with the generation telescopes will provide the new information of distance objects and the EBL density.

Acknowledgment: The Fermi data used in this work were obtained through the High Energy Astrophysics Science Archive Research Center (HEASARC), provided by NASA ' s Goddard Space Flight Center. Part of this work is based on archival data provided by the ASI Science Data Center (ASDC). We furthermore acknowledge use of archival Fermi and ASDC data.

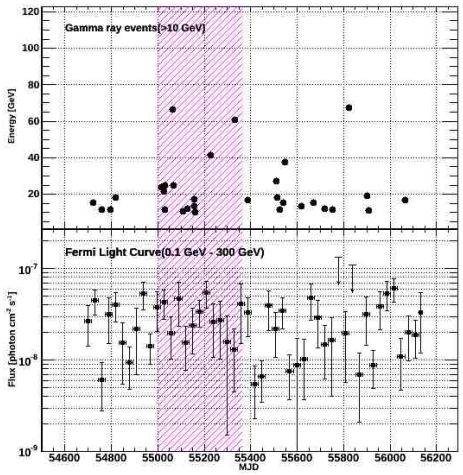

Fig. 2: PKS 0118-272. Top: Energy of 10-300GeV events over 10GeV in ROI of 0.26 degree (10GeV PSF) centered at the position of PKS 0118-272. Bottom: 0.1-300 GeV monthly light curve from 2008 August 05 to 2012 August 05. The arrows are the 3σ upper limits. Magenta region is the active period between MJD 55000 and MJD 55365, and it is used by SED of Fig.3.

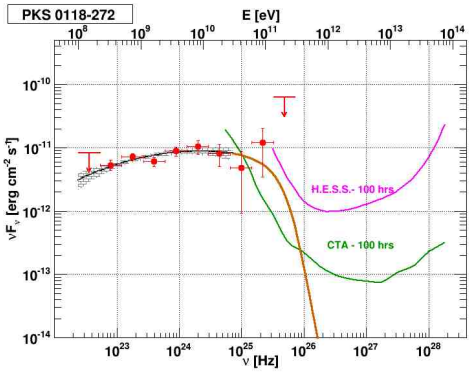

Fig. 3: Spectrum of PKS 0118-272 from MJD 55000 to MJD 55365. Black line and Black fill represent a best fit of log-parabolic model spectrum and best fit error region in the 0.1-20 GeV band (intrinsic spectrum). Red line represents an absorbed spectum on the EBL from [5]. Red points represents data points and a 3σ upper limit. Magenta and green line is the H.E.S.S.- I and the CTA sensitivity model by [7].

5. http://www.tmt.org/
6. http://www.gmto.org/
7. http://www.eso.org/sci/facilities/eelt/owl/

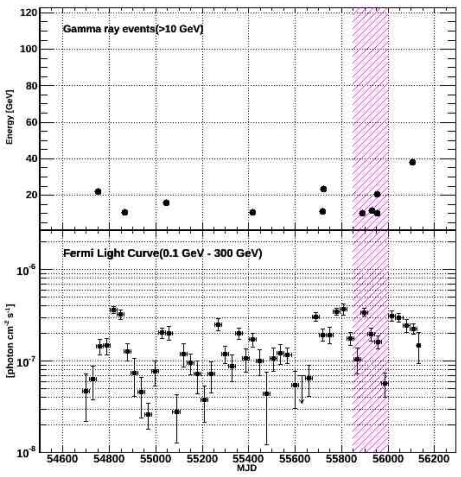

Fig. 4: PKS 1244-255. Notations are the same as Fig.4. Magenta region is the active period between MJD 55850 and MJD 56000, and it is used by SED of Fig.5.

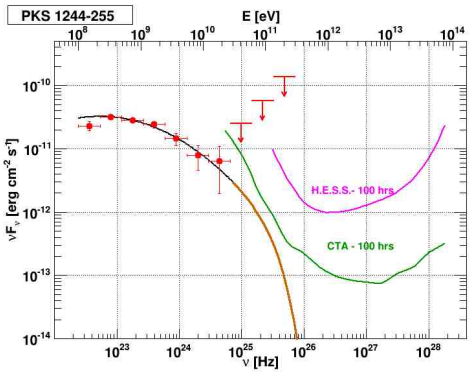

Fig. 5: Spectrum of PKS 1244-255 from MJD 55850 to MJD 56000. Notations are the same as Fig.4.

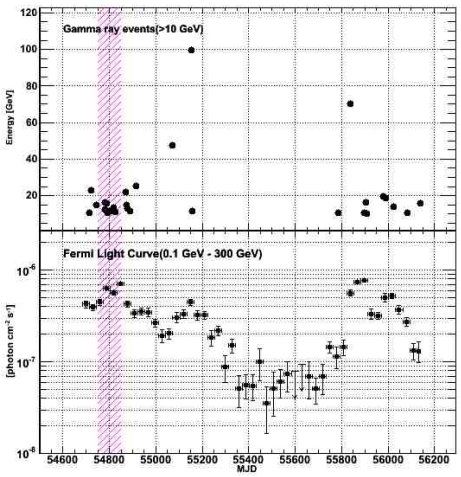

Fig. 6: PKS 0454-234. Notations are the same as Fig.4. Magenta region is the active period between MJD 54750 and MJD 54850, and it is used by SED of Fig.7.

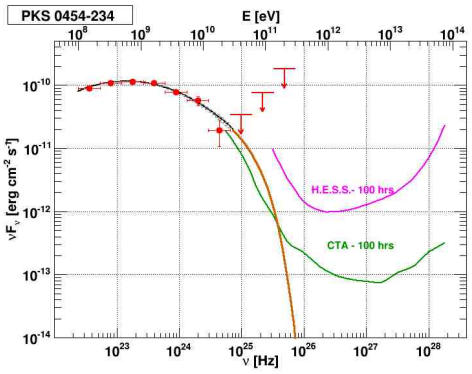

Fig. 7: Spectrum of PKS 0454-234 from MJD 54750 to MJD 54850. Notations are the same as Fig.3.

References

[1] M. Ackermann et al., The Astrophysical Journal **743**(2011) 171 doi:10.1088/0004-637X/743/2/171.
[2] J. Albert et al., Science **320**(2008) 1752-1754 doi:10.1126/science.1157087.
[3] L. Carrasco et al., Atel **#4647**, (2012).
[4] E. Cavazzuti, et al., ATel **#1898**, (2009).
[5] A. Domínguez et al., MNRAS **410**(2011), 2556-2578 doi:10.1111/j.1365-2966.2010.17631.x
[6] A. Franceschini, G. Rodighiero, M. Vaccari, A&A **487**(2008) 837-852 doi:10.1051/0004-6361:200809691.
[7] S. Funk, et al., Astropart.Phys. **43**(2013) 348-355 doi:10.1016/j.astropartphys.2012.05.018.
[8] M. Gaylard, et al., ATel **#3713**, (2011).
[9] R. Gilmore, et al., MNRAS **422**(2012) 3189-3207 doi:10.1111/j.1365-2966.2012.20841.x.
[10] F. Hungwe, et al., ATel **#3703**, (2011).
[11] A. Neronov, et al., **arXiv:arXiv:1207.1962**(2012).
[12] R. Nesci, ATel **#3722**, (2011).
[13] A. Savage, et al., MNRAS **177**(1976) 77-81.
[14] M. Stickel, et al., A&A **80**(1989) 103-114.
[15] A. Tramacere, N. Rea, ATel **#1894**, (2009).
[16] G. Vladilo, et al., A&A **327**(1997), 47-56.